Simplified Local Density Model for Adsorption over Large Pressure Ranges

Bharath Rangarajan, Carl T. Lira, and Ramkumar Subramanian
Dept. of Chemical Engineering, Michigan State University, East Lansing, MI 48824

A mean-field model is developed that superimposes the fluid-solid potential on a fluid equation of state to predict adsorption on a flat wall from vapor, liquid, and supercritical phases. A van der Waals-type equation of state is used to represent the fluid phase, and is simplified with a local density approximation for calculating the configurational energy of the inhomogeneous fluid. The simplified local density approximation makes the model tractable for routine calculations over wide pressure ranges. The model is capable of prediction of Type II and III subcritical isotherms for adsorption on a flat wall, and shows the characteristic cusplike behavior and crossovers seen experimentally near the fluid critical point.

Introduction

Physical adsorption of high-pressure fluids onto solids is of interest in the transportation and storage of fuel and radioactive gases; the separation and purification of lower hydrocarbons; solid-phase extractions; adsorbent regenerations using supercritical fluids (Tan and Liou, 1988, 1990); supercritical fluid chromatography (Strubinger and Parcher, 1989); and critical-point drying (Rangarajan and Lira, 1992). Understanding the thermodynamics and structure of the gas-solid interface is essential to the understanding of heterogeneous catalysis and wetting phenomena (Findenegg, 1983). While there are a large number of theoretical and experimental studies of adsorption below the critical temperature, there are few studies of adsorption near or above the critical temperature of the fluid. Such studies are especially relevant to the storage of methane at ambient temperatures ($T_r = 1.57$) at reasonably high densities.

Theoretical approaches to understanding and predicting adsorption range from simple empirical fits (Freundlich/Toth isotherms) to theoretically sound methods such as molecular dynamics (MD) and Monte Carlo (MC) simulations. Computer simulations such as the grand canonical ensemble Monte Carlo semiquantitatively predict the cusplike behavior near the critical point (van Megan and Snook, 1982). However, such methods are computationally intensive. Simulations are difficult near the critical point due to fluctuations, and require a large number of molecules and consequently significant amounts of supercomputer time. Statistical mechanical theories such as the density functional theory are also computationally intensive, although they are about two orders of magnitude faster than computer simulations (Gubbins, 1990). On the other hand, the traditional empirical and semiempirical methods that are computationally undemanding are unable to account for the wide variety of shapes of adsorption isotherms seen near the critical region.

Reliable experimental measurements of the adsorption of fluids onto well-characterized solids are essential in order to test the different theories of adsorption. One of the best adsorbents for this purpose is graphitized carbon black (g.c.b. or Graphon), which provides a molecularly smooth, nonporous, energetically homogeneous surface. Findenegg and coworkers have used graphitized carbon black and measured the high-pressure adsorption of a variety of gases including ethylene, propane, argon, and krypton at temperatures near and above the fluid critical temperature (Findenegg, 1983). Adsorption isotherms of ethylene on graphon in subcritical and supercritical regions are shown in Figure 1. Figure 2 shows adsorption isotherms of krypton on graphon at temperatures well above the critical temperature ($T_r = 1.2 - 1.78$). A wide variety of fascinating behavior is seen in adsorption isotherms in the near-critical and supercritical regions (Menon, 1968; Findenegg, 1983). To model the different behaviors in subcritical and supercritical adsorption isotherms, Findenegg and coworkers (1983) use the Frenkel-Halsey-Hill theory (Hill, 1952) to represent adsorption in the subcritical region and a corresponding states argument for the supercritical region.

Correspondence concerning this article should be addressed to C. T. Lira.

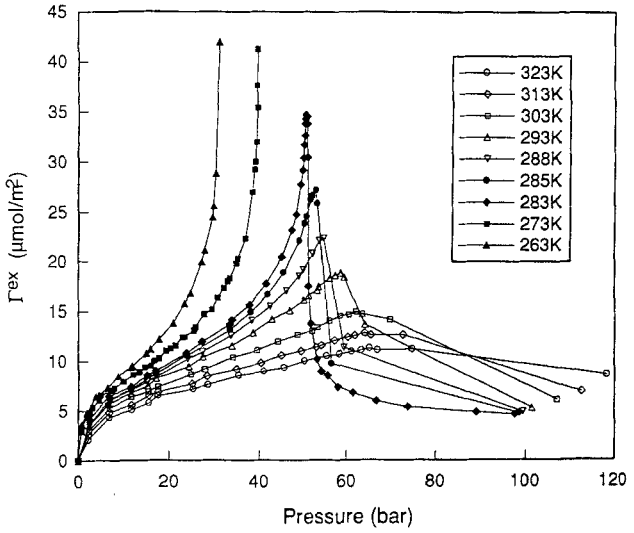

Figure 1. Surface excess of ethylene on graphitized carbon black as reported by Findenegg (1983).

Figures 1 and 2 demonstrate crossovers of the adsorption isotherms of pure fluids above the critical pressure. Consequently, this behavior plays an important role in the design of supercritical fluid adsorbers/desorbers. Tan and Liou (1988, 1990) found that for carbon in equilibrium with toluene and supercritical CO_2 there are crossovers of the equilibrium toluene loadings at different temperatures, which occur above the critical pressure of CO_2. As the bulk concentration of toluene is increased, the crossovers shift to higher pressures. Akman and Sunol (1991) using the Toth equation for the adsorbed phase and a cubic equation of state for the fluid phase modeled such fixed-bed supercritical desorbers. Simple models that can predict such crossovers will be extremely useful in the design of fixed-bed adsorbers/desorbers and in the field of supercritical fluid technology.

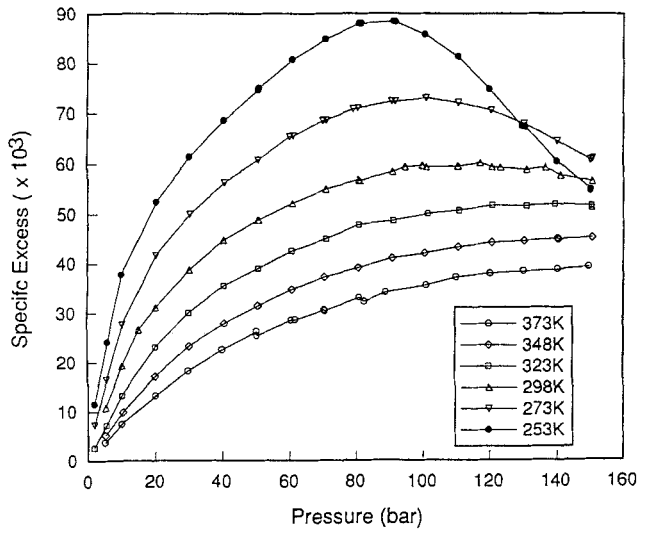

Figure 2. Specific surface excess (mass adsorbed per mass of solid) for krypton on graphitized carbon black as reported by Findenegg (1983).

The focus of this article is to develop a simplified-local-density (SLD) model, and demonstrate its application in predicting pure fluid adsorption isotherms over wide pressure and temperature ranges. The SLD model developed in this work superimposes the fluid-solid interaction potential on the van der Waals equation of state. Our intention is to present the concepts necessary to adapt common cubic equations of state for describing the adsorption phenomenon. The SLD model is intended to bridge the gap between the computationally intensive but theoretically sound statistical mechanical models and the undemanding, empirical methods. The SLD concept should be a useful engineering supplement to other available models, and is not intended as a replacement for the statistical mechanical models. In the next section we describe the model, its solution, then briefly discuss various limiting cases. Model predictions are compared with experimental data from literature. Finally, we discuss some of the limitations of this model, and suggest improvements utilizing more accurate mean-field models.

Model Development

While adsorption is expressed in several different ways, it is unambiguously defined by the surface excess (Γ^{ex}), the excess number of moles per unit area of adsorbent. The surface excess is defined as

$$\Gamma^{ex} \equiv \int_{z_0}^{\infty} (\rho(z) - \rho_{\text{bulk}})\, dz \tag{1}$$

where $\rho(z)$ is the molar density of the fluid at a distance z from the surface of the solid, and ρ_{bulk} is the bulk density of the fluid. Bulk fluid is defined as fluid far from the adsorption surface, where the fluid-solid potential is zero. The lower limit of integration is the surface of the solid, and is taken as the plane at $z_0 = \sigma_{ff}/2$. The surface excess is sometimes expressed as the excess number of moles per unit mass of adsorbent.

The model developed here has a basis similar to the Polyani potential theory, where the adsorbent exerts an attractive potential on the adsorbate. The model is also similar to the approaches of Barrer and Robins (1951), Hill (1949), Sullivan (1979), and Kung et al. (1990). The attractive potential between the fluid and solid, at any point z, is assumed to be independent of temperature and the number of molecules at and around that point. At equilibrium, the molar chemical potential μ is calculated by contributions from fluid-fluid and fluid-solid interactions

$$\mu = \mu_{\text{bulk}} = \mu_{ff}(z) + \mu_{fs}(z) \tag{2}$$

where the subscript "bulk" refers to the bulk fluid, the subscript *ff* to the fluid-fluid interactions, and the subscript *fs* to the fluid-solid interactions. Equation 2 requires that at a distance z from the wall, the sum of the chemical potential due to the fluid-fluid interactions and the attractive potential exerted by the solid on the fluid remains constant. While such an equation has been written from the principles of chemical equilibrium for a gravitational field (Denbigh, 1981), this fundamental result has also been derived by minimizing the grand

potential (Evans, 1979; Rowlinson and Widom, 1982; Davis and Scriven, 1982).

If the fluid-solid potential per molecule is $\Psi(z)$, then the molar fluid-solid potential is given by

$$\mu_{fs}(z) = N_A \Psi(z) \tag{3}$$

where N_A is Avogadro's number. Therefore

$$\mu_{ff}(z) = \mu_{\text{bulk}} - N_A \Psi(z). \tag{4}$$

For a nonideal bulk fluid

$$\mu_{\text{bulk}}(T) = \mu_0(T) + RT \ln(f_{\text{bulk}}/f_0) \tag{5}$$

where f_{bulk} is the bulk fugacity and f_0 is a reference fugacity. For an inhomogeneous fluid,

$$\mu_{ff}(z) = \mu_0(T) + RT \ln[f_{ff}(z)/f_0] \tag{6}$$

where $f_{ff}(z)$ is the fluid-fluid contribution to the fugacity of the fluid at a position z. Equations 4, 5, and 6 lead to

$$f_{ff}(z) = f_{\text{bulk}} \exp[-\Psi(z)/(kT)]. \tag{7}$$

It should be noted that $\Psi(z)$ is negative when attractive, leading to an increased fugacity near the wall. The fluid chemical potential consists of a repulsive contribution μ_{rep} and an attractive contribution μ_{att} (Vera and Prausnitz, 1972),

$$\mu_{ff} = \mu_{\text{rep}} + \mu_{\text{att}}. \tag{8}$$

For a homogeneous fluid, using the van der Waals equation of state

$$\mu_{\text{rep}} = RT\{\ln[RT/(\nu - b)] + b/(\nu - b)\} \tag{9}$$

where ν is molar volume and b is the van der Waals constant. The attractive potential is given by

$$\mu_{\text{att}} = \int_V \phi(r) \frac{g(r)}{\nu} dV \tag{10}$$

where V denotes the volume of integration (all space occupied by the fluid), $\phi(r)$ the two-body interaction potential, and $g(r)$ the radial distribution function, which is taken to be a constant outside the hard-sphere diameter for a van der Waals fluid (McQuarrie, 1976). In the case of a homogeneous fluid ($\nu \neq \nu(z)$) Eq. 10 simplifies to the common form

$$\mu_{\text{att}} = \frac{-2a_{\text{bulk}}}{\nu} \tag{11}$$

where a_{bulk} is the van der Waals constant. In order to evaluate the integral in Eq. 10 for an inhomogeneous fluid, if the density changes with position more gradually than $\phi(r)$ does, then one needs to include density as a function of position. Equation 10 suggests that a feasible approximation might be to use a density at the local position for evaluation of the integral. In other words, the fluid at point z is treated as a homogeneous fluid at a density of $\rho(z)$ [such an approximation is the one used by Barrer and Robins (1951)]. Since the two-body potential $\phi(r)$ is short-ranged ($\propto 1/r^6$), and the product of $\phi(r)$ and $\rho(z)$ appears in the configurational integral (Eq. 10), it seems reasonable that most of the value of the integral (at z) results from contributions of $\phi(r)$ and $\rho(z)$ near z. Far from the given point z, where $\rho(z)$ changes, the two-body potential ($\phi(r)$) will approach zero. Since the density of the fluid is larger closer to the attractive wall and smaller farther away from the wall, some of the errors introduced by this approximation cancel, although the approximation will not be as good near a phase transition. The term "local" refers to the fact that all thermodynamic properties at point z are calculated using a single density value, $\rho(z)$, a "local average" density, and are not calculated from gradients in density about the point z. This approximation is called the local density approximation.

Using an equation of state, an expression for fugacity in terms of the molar density or volume can be derived. The van der Waals equation of state leads to the following expression for fugacity for a homogeneous fluid:

$$f_{\text{bulk}} = RT/(\nu - b) \exp[b/(\nu - b) - 2a_{\text{bulk}}/(\nu RT)]. \tag{12}$$

For an inhomogeneous fluid, the problem is one of calculating the density profile $\rho(z)$ that satisfies Eq. 7. Following Hill (1951), Sullivan (1979), and Kung et al. (1990) we assume the short-range repulsive forces determine μ_{rep} by the local density. If we assume that μ_{att} is also determined by the density of $\rho(z)$ (local density approximation), then we can rewrite Eq. 12 to calculate density as a function of z

$$f_{ff}(z) = RT/[\nu(z) - b] \exp\{b/[\nu(z) - b] - 2a(z)/[\nu(z)RT]\} \tag{13}$$

where $a(z)$ is evaluated from the integral given in Eq. 10, in which the molar volume in the denominator is approximated by the local molar volume at z. In the model of Barrer and Robins (1951), the van der Waals a is independent of z, [$a(z) = a_{\text{bulk}}$]. In the present model, for a flat wall, we exclude from the integral of Eq. 10 that portion of space occupied by the solid adsorbent. This leads to the following expressions for $a(z)$ (see the Appendix):

$$a(z) = a_{\text{bulk}} \left(\frac{5}{16} + \frac{6}{16} \frac{z}{\sigma_{ff}} \right) \quad \text{for} \quad 0.5 \leq \frac{z}{\sigma_{ff}} \leq 1.5 \tag{14}$$

$$a(z) = a_{\text{bulk}} \left[1 - \frac{1}{8\left(\frac{z}{\sigma_{ff}} - \frac{1}{2} \right)^3} \right] \quad \text{for} \quad 1.5 \leq \frac{z}{\sigma_{ff}} < \infty \tag{15}$$

where

$$a_{\text{bulk}} = \frac{27}{64} \frac{R^2 T_c^2}{P_c}. \tag{16}$$

Algorithm for Determination of Density Profile

Given a bulk fluid pressure and temperature, the bulk density and bulk fugacity are calculated. Since the fluid-wall potential is chosen, Eq. 7 provides the fugacity at a point z, $f_{ff}(z)$. The value of the van der Waals $a(z)$ is calculated from Eqs. 14–16. Equation 13 is then solved iteratively for $\nu(z)$. Below the critical point there may be three values of ν that will satisfy Eq. 14, and the stable root is the root that gives the highest pressure. These calculations are performed over z and the surface excess is then generated from Eq. 1. A FORTRAN program capable of generating adsorption isotherms is available (Rangarajan, 1992), and may be obtained from the authors. At a given temperature, this program utilizes the critical temperature and pressure of the fluid, the fluid-solid interaction potential, and the size of the fluid and solid molecules to calculate the surface excess as a function of pressure, and the density as a function of position.

Results

The SLD model discussed here superimposes the attraction of the fluid molecules to the wall onto the attraction of fluid molecules to one another. The asymmetry of fluid-fluid interactions near an inert wall is incorporated into the equations for a, the attractive constant. At an inert wall [$z = 0.5\sigma_{ff}$, $\Psi(z) = 0$], these calculations predict that $a_{\text{wall}} = a_{\text{bulk}}/2$, which when combined with Eq. 16 leads to $T_{c\,\text{wall}} = T_{c\,\text{bulk}}/2$, the mean field prediction of the two-dimensional van der Waals model of deBoer (1953). Several other limiting cases are discussed below and compared with theory, computer simulations, and experiments.

Ideal gas – hard wall

For an ideal gas and hard wall, there are neither fluid-fluid intermolecular attractions, nor fluid-wall attractive forces: Therefore, $a = 0$, $b = 0$, and $\Psi(z) = 0$, $f = P$, and Eq. 7 reduces to $P(z) = P_{\text{bulk}}$. When combined with the ideal gas law this reduces to $\rho(z) = \rho_{\text{bulk}}$, and as expected there is no adsorption.

Ideal gas – attractive wall

Here $a = 0$, $b = 0$, $f = P$. Equation 7 exactly reduces to $P(z) = P_{\text{bulk}} \exp[-\Psi(z)/(kT)]$. With the ideal gas law this gives $\rho(z) = \rho_{\text{bulk}} \exp[-\Psi(z)/(kT)]$. The surface excess is

$$\Gamma^{ex} = \int_{z_0}^{\infty} (\rho(z) - \rho_{bulk})\, dz$$

$$= \rho_{bulk} \int_{z_0}^{\infty} \{\exp[-\Psi(z)/(kT)] - 1\}\, dz. \quad (17)$$

Since the integral is constant, and ρ_{bulk} proportional to the pressure P_{bulk}, this leads to Henry's law.

Attractive fluid – hard wall

For an attractive fluid and hard wall, $a > 0$, $b > 0$, and $\Psi(z) = 0$, $f(z) = f_{\text{bulk}}$. The model predicts a reduced density near the wall, because of attraction of the fluid molecules near the wall to fluid molecules in the bulk. In fact a vapor-liquid phase transition is seen adjacent to the wall for certain cases when the bulk fluid is liquid. This is similar to the observations of Abraham and Singh (1978).

Table 1. Molecular Properties Used in SLD Model

System	σ_{ff}(nm)	σ_{fs}(nm)	ϵ_{fs}/k(K)
Ethylene-graphon	42.2	38.1	450, 23
Krypton-graphon	35	34.5	225

Attractive fluid – attractive wall

For this case, $a > 0$, $b > 0$, $\Psi(z) < 0$. In general, for an attractive fluid near an attractive wall an increase in density is exhibited near the wall, depending on the magnitude of $\Psi(z)$. If the wall-fluid forces are stronger than the fluid-fluid forces, the fluid will wet the wall; otherwise there will be a rarefaction of gases near the wall. To represent the interactions of the adsorbate and adsorbent we have chosen the partially integrated 10–4 potential model (Lee, 1988)

$$\Psi(z) = 4\pi\rho_{\text{atoms}}\epsilon_{fs}\sigma_{fs}^6\left(\frac{\sigma_{fs}^6}{5x_1^{10}} - \frac{1}{2}\sum_{i=1}^{4}\frac{1}{x_i^4}\right) \quad (18)$$

where $\rho_{\text{atoms}} = 0.382$ atoms/Å^2 and x_i is the intermolecular distance between fluid molecular centers and the ith plane of solid molecules. We have truncated the interactions at the fourth plane of solid atoms, where the interplanar spacing is 3.35 Å. Table 1 summarizes other parameters used in this work. Note that ϵ_{ff} is not tabulated because the fluid-fluid contribution is calculated from Eqs. 14–16 and not directly from ϵ_{ff}. Steele (1974), Nicholson and Parsonage (1982), and Lee (1988) offer a further discussion of fluid-solid potentials.

Figure 3 shows adsorption isotherms that were calculated using the 10–4 potential of Eq. 18 and the parameters for ethylene and graphon in Table 1. The curves are qualitatively similar to Figure 1. A knee is present, the magnitude of which can be increased by increasing the solid-fluid interaction energy ϵ_{fs} (Figure 3 also shows calculated adsorption isotherms for condensed phases at subcritical temperatures above the bulk vapor pressure that are not present in Figure 1). Some characteristic features of adsorption of near-critical fluids are the cusp-shaped isotherms seen near the critical point, and the "crossover" of adsorption isotherms at different temperatures. Consider the effect of temperature at a fixed pressure below the critical pressure. Below the critical pressure, adsorption decreases with increasing temperature, but this trend is reversed above the crossover region at pressures above the critical pressure. The crossover of the isotherms is eliminated by plotting the calculated surface excess with respect to calculated bulk density as shown in Figure 4. The reason for the cusplike behavior of a supercritical isotherm in Figure 3 can be understood from the calculated density profiles shown in Figure 5. Below the critical pressure region, the adsorbed layer increases in thickness faster than the bulk density increases. Above the critical pressure region, the bulk fluid becomes increasingly incompressible, and the bulk fluid density approaches the density of the adsorbed fluid, causing the surface excess to decrease.

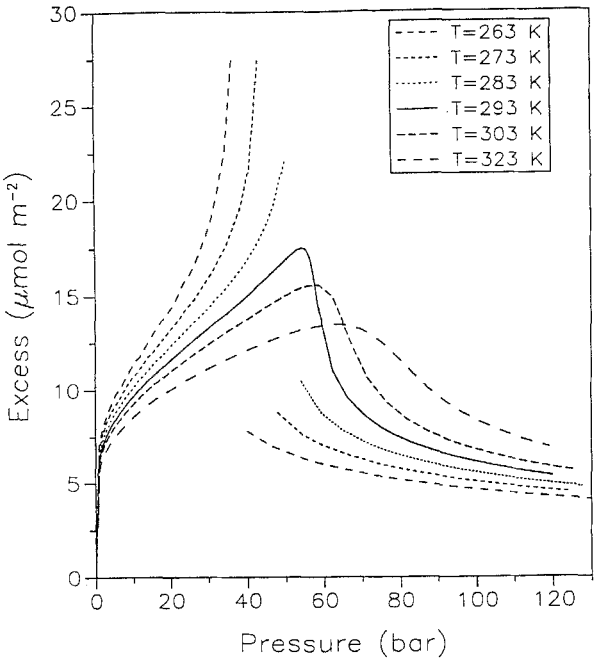

Figure 3. Surface excess of ethylene on graphitized carbon black as predicted by the SLD model using parameters in Table 1.

The critical temperature of ethylene is 282.4 K.

Type III isotherms are normally observed when the attraction between the solid and fluid is weak. Figure 6 demonstrates the capability of the SLD model for prediction of Type III isotherms. In this case, the fluid parameters are for ethylene, but the magnitude of the ϵ_{fs} has been decreased. The smaller ϵ_{fs} results in elimination of the knee and yields a Type III adsorption isotherm. At very low pressures and temperatures, a discontinuity in the adsorption isotherms is predicted (not shown here), indicating a phase transition in the adsorbed phase similar to those discussed for a two-dimensional model (Ross and Olivier, 1964). At high pressures,

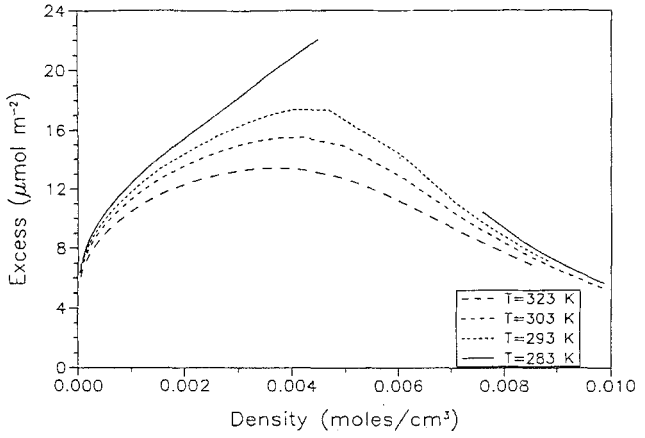

Figure 4. Surface excess of ethylene on graphitized carbon black from Figure 3 replotted with bulk density.

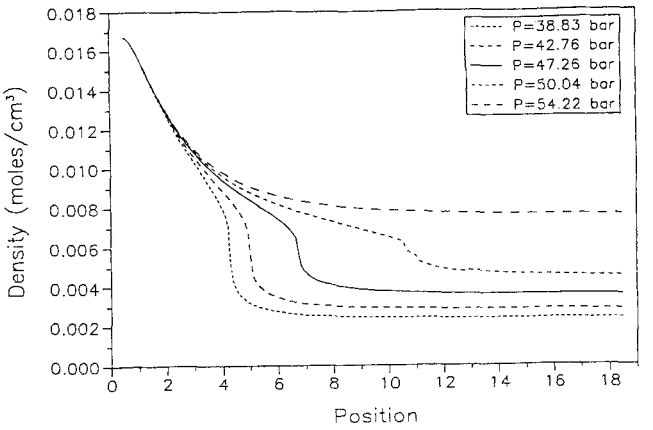

Figure 5. Density profiles from SLD model for ethylene on graphitized carbon black as predicted by the SLD model at a temperature of 283 K.

The position is measured by z/σ_f.

when the bulk fluid exists as a liquid, the SLD model can predict a negative surface excess when ϵ_{fs} is small. Negative surface excesses have also been predicted by Sullivan (1979). Figure 7 shows some predicted adsorption isotherms of krypton on graphon, at temperatures far above the critical temperature. When compared with experimental data shown in Figure 2, the predictions are again qualitatively correct. This model predicts some gas-liquid transitions on the surface, similar to the transitions seen in the experiments of Thomy (Bienfait, 1980).

Discussion

There are a number of methods used to predict adsorption, and these methods range from simple empirical fits to fundamentally sound molecular simulations. One of the most popular empirically adjusted models for adsorption is the Langmuir isotherm, a two-parameter equation. The Langmuir equation is only valid for monolayer adsorption, and therefore predicts only Type I isotherms. The Brunauer-Em-

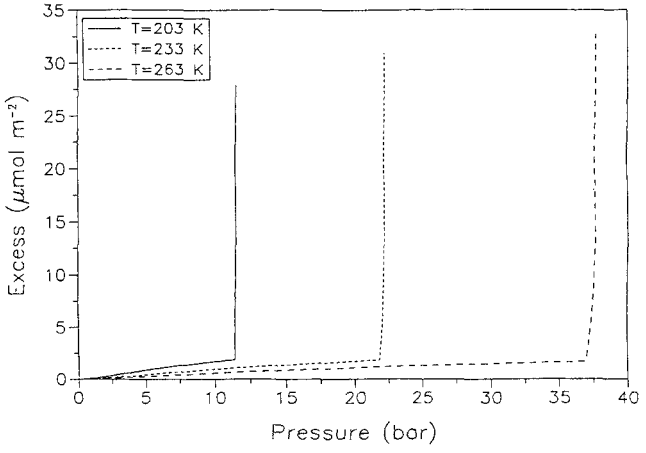

Figure 6. SLD model showing Type III behavior.

Parameters are as for Figure 3 except ϵ_{fs}/k = 23 K.

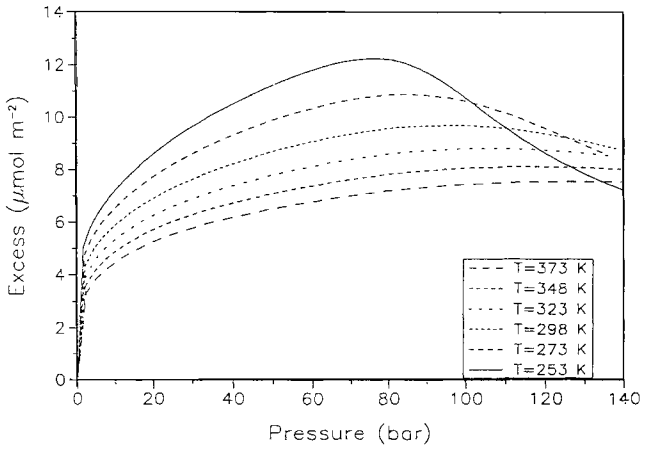

Figure 7. SLD model for surface excess of krypton on graphitized carbon black using parameters from Table 1.

The critical temperature of krypton is 209.4 K.

met-Teller (BET) theory extends the Langmuir theory to multilayers. However, some of its limitations are due to the assumptions made in developing the theory: (1) the surface is energetically homogeneous; (2) there are no lateral adsorbate interactions; (3) adsorption is localized–adsorbed molecules are fixed on sites and do not laterally move; (4) the heat of adsorption in the second and higher layers is the same as the heat of condensation. Most of these assumptions are valid for pressures in the range $0.05 < P/P^s < 0.35$, where the high energy sites are filled but extensive multilayer condensation has not commenced. The BET theory is limited to subcritical temperatures, and assumes an ideal gas vapor phase, although corrections can be applied.

A different approach treats the adsorbed phase as a two-dimensional fluid, and uses a two-dimensional equation of state to represent the adsorbed layer (Hill, 1946, 1947, 1948; de Boer, 1953). The two-dimensional equations of state allow for interactions between fluid molecules in the first adsorbed layer. Neither the Langmuir nor the BET theory allow for interactions between molecules, either on the surface or between molecules in different layers.

The simplified local density model builds on these various approaches. By treating the fluid with a van der Waals equation with a suitably modified a, the SLD model allows for interactions between adsorbed molecules at various distances from the wall. All of the models mentioned earlier (including ours) assume an energetically homogeneous surface. The effect of heterogeneity will be pronounced at extremely low pressures and coverages, where the high energy sites are unfilled. To represent a heterogeneous surface, one could fit the potential to adsorption in the Henry's law region, and then work with a pseudohomogeneous surface.

The limitations of the model can be attributed to (1) the lack of structure in the fluid; (2) the use of the local density approximation; and (3) the use of the van der Waals equation to describe the fluid properties. Since we are using the van der Waals equation and a mean field approach, we do not predict any of the fluid structure seen using either computer simulations or density functional theory (Snook and Henderson, 1978; Vanderlick et al., 1988; Kierlik and Rosinberg, 1991). This model cannot describe discrete fluid structure or be used to study packing near a wall. The use of the local density approximation also results in the physically unrealistic prediction of abrupt vapor-liquid interfaces. Despite the fundamental theoretical limitations of the model, since model predictions mimic experimental trends, this model may be acceptable for engineering calculations. In order to estimate the errors introduced by the use of the local density approximation, Eq. 10 was solved keeping the density inside the integral, leading to an integral equation (IE) (Pyada, 1994). When compared, solutions to the SLD model and IE approach showed differences that were dependent on pressure, temperature, and magnitude of the gas-solid interaction potential. For the adsorption of ethylene on graphon, the SLD model tends to underpredict adsorption (relative to the integral equation (IE)) by about 10–20% between $0.9 < T_r < 1.1$, except where the surface excess increases steeply at high pressures. At pressures near 1 bar, the differences are less than 1%. These comparisons show that the local density assumption can provide a reasonably approximate solution to the adsorption problem.

A limitation of the van der Waals-based SLD model is the fact that predicted magnitudes of adsorption and vapor pressures are incorrect. For accurate prediction, the equation of state must be able to correctly predict the vapor pressure and liquid density. The inaccuracies of the van der Waals equation in this regard are well documented. In order to represent the fluid properties any equation of state can be used, provided the repulsive and configurational contributions can be separated for use in Eq. 7. The selection of the van der Waals equation as the basis of this work was due to the fact that it is the simplest and most easily adapted equation of state with a theoretical basis. The objective of this work is to demonstrate that the proposed approach provides qualitative predictions with the van der Waals equation, and lay down the framework required to use a more accurate equation of state. A comparison of Figures 1 and 3 shows that the SLD model exhibits poor prediction of the vapor pressure for subcritical isotherms, but does better at predicting the pressure of the maxima in the supercritical isotherms. This is because the van der Waals parameters a and b were obtained from the critical temperature and pressure. The ϵ_{fs} in Table 1 have been selected to provide a semiquantitative fit to the magnitude of experimental adsorption.

Future work will incorporate equations of state that are more capable of representation of fluid properties for engineering calculations. In fact, preliminary results using the Peng-Robinson equation of state show improved accuracy in predicting the magnitude of adsorption using temperature-independent parameters (Pyada, 1994). Cubic equations are widely used in industry, and a method that adapts them to the adsorption problem could find widespread use in process calculations. Future work will also address extension of the model to Type I, IV, and V isotherms, and multicomponent mixtures.

The SLD model serves as a good first approximation and can provide rapid surveys of adsorption behavior to guide more detailed and time-consuming simulations. This model is not intended to replace any of the more complete theories such as Monte Carlo simulations, molecular dynamics, or

density functional theory, but instead provides a simple and approximate solution to the adsorption problem. The model may be viewed as a compromise or a bridge between the 2-D van der Waals model, Frenkel-Halsey-Hill theory, and more rigorous density functional or integral equation approaches.

Conclusions

A simple model based on spatial invariance of chemical potential, along with a cubic equation of state can model a variety of adsorption isotherms over large pressure and temperature ranges. The SLD model provides information about the density profile of the adsorbed fluid. Under certain conditions the SLD model may predict phase transitions at the surface and transitions between adsorbed layer and bulk fluid, or may predict negative adsorption. In the subcritical region the SLD model predicts Type II and III isotherms on flat walls. In the supercritical region the model shows the experimentally observed cusplike behavior near the critical pressure, as well as the crossovers seen experimentally at higher pressures. Future work will address quantitative modeling of adsorption.

Notation

k = Boltzmann's constant
P, P^s = pressure, vapor pressure
T = temperature
z_0 = distance of closest approach to fluid to wall

Subscripts

c = critical state
f = fluid property
hs = hard-sphere contribution

Literature Cited

Abraham, F. F., and Y. Singh, "Comment on the Structure of a Hard Sphere Fluid in Contact with a Soft Repulsive Wall," *J. Chem. Phys.*, **68**, 4767 (1978).

Akman, U., and A. K. Sunol, "Modeling of Supercritical Desorbers with an Equation-of-State-Based Isotherm," *AIChE J.*, **37**, 215 (1991).

Barrer, R. M., and A. B. Robins, "Multi-layer Sorption in Terms of an Equation of State," *Trans. Farad. Soc.*, **47**, 773 (1951).

Bienfait, M., "Two-Dimensional Phase Transition in Classical van der Waals Films Adsorbed on Graphite," *Phase Transitions in Surface Films*, J. G. Dash and J. Ruvalds, eds., Plenum Press, New York, 29 (1980).

Davis, H. T., and L. E. Scriven, "Stress and Structure in Fluid Interfaces," *Advances in Chemical Physics*, Vol. 49, I. Prigogine and S. A. Rice, eds., Wiley, New York, 357 (1982).

deBoer, J. H., *The Dynamical Character of Adsorption*, Clarendon Press, Oxford (1953).

Denbigh, K., *The Principles of Chemical Equilibrium*, 4th ed., Cambridge Univ. Press, Cambridge, England (1981).

Evans, R., "The Nature of Liquid-Vapor Interface and Other Topics in the Statistical Mechanics of Non-Uniform Classical Fluids," *Adv. Phys.*, **28**, 143 (1979).

Findenegg, G. H., "High-Pressure Physical Adsorption of Gases on Homogeneous Surfaces," *Fundamentals of Adsorption*, A. L. Myers and G. Belfort, eds., Engineering Foundation, New York, 207 (1983).

Gubbins, K. E., "Molecular Adsorption in Micropores," *Chem. Eng. Prog.*, **86**(8), 42 (1990).

Hill, T. L., "Statistical Mechanics of Multi-Molecular Adsorption: II. Localized and Mobile Adsorption and Absorption," *J. Chem. Phys.*, **14**, 441 (1946).

Hill, T. L., "Statistical Mechanics of Multi-Molecular Adsorption: III. Introductory Treatment of Horizontal Interactions: Capillary Condensation and Hysteresis," *J. Chem. Phys.*, **15**, 767 (1947).

Hill, T. L., "Statistical Mechanics of Multi-Molecular Adsorption: IV. The Statistical Analog of the BET Constant a_1b_2/b_1a_2. Hindered Rotation of a Symmetrical Diatomic Molecule Near a Surface," *J. Chem. Phys.*, **16**, 181 (1948).

Hill, T. L., "Physical Adsorption and the Free Volume Model for Liquids," *J. Chem. Phys.*, **17**, 590 (1949).

Hill, T. L., "Liquid-Vapor Transition Region and Physical Adsorption According to van der Waals Equation," *J. Chem. Phys.*, **19**, 261 (1951).

Hill, T. L., "Theory of Physical Adsorption," in *Advances in Catalysis*, Vol. IV, W. G. Frankenburg, E. K. Rideal, V. I. Komarewsky, eds., Academic Press, New York, 211 (1952).

Kierlik, E., and M. L. Rosinberg, "Density-Functional Theory for Inhomogeneous Fluids: Adsorption of Binary Mixtures," *Phys. Rev. A*, **44**, 5025 (1991).

Kung, W. C., L. E. Scriven, and H. T. Davis, "Wetting Transitions and Surface Critical Phenomena at Solid-Fluid Interfaces," *Chem. Phys.*, **149**, 141 (1990).

Lee, L. L., *Molecular Thermodynamics of Non-Ideal Fluids*, Butterworths, Stoneham, MA (1988).

McQuarrie, D. A., *Statistical Mechanics*, Harper & Row, New York, 304 (1976).

Menon, P. G., "Adsorption at High Pressures," *Chem. Rev.*, **68**, 277 (1968).

Nicholson, D., and N. G. Parsonage, *Computer Simulation and the Statistical Mechanics of Adsorption*, Academic Press, New York (1982).

Pyada, H., "A Local Density Approximation for Adsorption," MS Thesis, Michigan State Univ., East Lansing (1994).

Rangarajan, B., "Shrinkage Characterization in the Production of Aerogels and a Model for Physical Adsorption of Fluids on Solids–From Vacuum to Supercritical Conditions," PhD Thesis, Michigan State Univ., East Lansing (1992).

Rangarajan, B., and C. T. Lira, "Interpretation of Aerogel Shrinkage During Drying," *Better Ceramics Through Chemistry V*, M. J. Hampden-Smith, W. G. Kemperer, and C. J. Brinker, eds., Materials Research Society, Pittsburgh, 559 (1992).

Ross, S., and J. P. Olivier, *On Physical Adsorption*, Interscience, New York (1964).

Rowlinson, J. S., and B. Widom, *Molecular Theory of Capillarity*, Clarendon Press, Oxford (1982).

Snook, I. K., and D. Henderson, "Monte Carlo Study of a Hard-Sphere Fluid Near a Hard Wall," *J. Chem. Phys.*, **68**, 2134 (1978).

Steele, W. A., *The Interaction of Gases with Solid Surfaces*, Pergamon Press, Oxford (1974).

Strubinger, J. R., and J. F. Parcher, "Surface Excess (Gibbs) Adsorption Isotherms of Supercritical Carbon Dioxide on Octadecylbonded Silica Stationary Phases," *Anal. Chem.*, **61**, 951 (1989).

Sullivan, D. E., "van der Waals Model of Adsorption," *Phys. Rev. B.*, **20**, 3991 (1979).

Tan, C.-S., and D.-C. Liou, "Desorption of Ethyl Acetate from Activated Carbon by Supercritical Carbon Dioxide," *Ind. Eng. Chem. Res.*, **27**, 988 (1988).

Tan, C.-S., and D.-C. Liou, "Adsorption Equilibrium of Toluene from Supercritical Carbon Dioxide on Activated Carbon," *Ind. Eng. Chem. Res.*, **29**, 1412 (1990).

Vanderlick, T. K., L. E. Scriven, and H. T. Davis, "Molecular Theory of Confined Fluids," *J. Chem. Phys.*, **90**, 2422 (1989).

van Megan, W., and I. K. Snook, "Physical Adsorption of Gases at High Pressures. 1. The Critical Region," *Mol. Phys.*, **45**, 6 (1982).

Vera, J. H., and J. M. Prausnitz, "Generalized van der Waals Theory for Dense Fluids," *Chem. Eng. J.*, **3**, 1 (1972).

Appendix: van der Waals Equation and Configurational Energy Calculations

If we consider a canonical ensemble, the partition function Q is given by (Vera and Prausnitz, 1972)

$$Q = \frac{1}{N!} V_f^N \left(\exp - \frac{\Phi}{2kT} \right)^N \left(\frac{q_{r,v,e}}{\Lambda^3} \right)^N$$

where $\Lambda = h/(2\pi mkT)^{1/2}$. The Helmholtz energy A and the pressure are related to the partition function:

$$P = -\left(\frac{\partial A}{\partial V}\right)_{T,N} = kT\left(\frac{\partial \ln Q}{\partial V}\right)_{T,N}$$
$$= kTN\frac{\partial \ln V_f}{\partial V} - \frac{N\partial\Phi/2}{\partial V}$$
$$= P_{\text{rep}} + P_{\text{att}}$$

where the molecular rotational, vibrational, electronic partition function, $q_{r,v,e}$, is assumed to have no volume dependence. The van der Waals free volume V_f, for a system with N molecules, is given by

$$V_f = V - \frac{N}{N_A}b.$$

The repulsive part of the pressure is

$$P_{\text{rep}} = kTN\frac{1}{V - \frac{N}{N_A}b} = \frac{RT}{v - b}.$$

If Φ is the sum of two-body interactions between an arbitrarily selected central molecule and all other molecules around it, $\phi(r)$ is the two-body interaction potential, and $g(r)$ the radial distribution function, then

$$\Phi = \int_0^\infty \frac{N}{V}\phi(r)g(r)4\pi r^2 dr.$$

For a van der Waals fluid, following McQuarrie (1976), $g(r) = 0$, for $r \le \sigma$, and $g(r) =$ constant, for $r > \sigma$, where σ is the hard-core radius of the fluid molecule. To simplify notation, the subscript ff is omitted from σ throughout the Appendix.

If we assume that the molecules interact with an infinite hard-core repulsive potential and an inverse-sixth attractive potential, then for $r > \sigma$,

$$\phi(r) = -\epsilon_{ff}\frac{\sigma^6}{r^6}$$

where ϵ_{ff} is the maximum energy of attraction between a pair of fluid molecules. In the bulk fluid, this leads to

$$\Phi_{\text{bulk}} = \frac{-4\pi\epsilon_{ff}\sigma^3 N_A}{3}\rho$$
$$a_{\text{bulk}} = 2\pi\epsilon_{ff}\sigma^3 N_A^2/3$$
$$P_{\text{att}} = -N\frac{\partial\Phi/2}{\partial V} = -\frac{2\pi\epsilon_{ff}\sigma^3 N_A^2}{3v^2} = -\frac{a}{v^2}.$$

Nonhomogeneous systems

Consider a fluid molecule of diameter σ at location z in the vicinity of a wall, where $0.5\sigma \le z \le 1.5\sigma$. For convenience of integration we define a cylindrical coordinate system with the origin at an arbitrary molecular center at z, let y be a dummy variable to denote axial distance and let r denote radial distance. The configurational energy can be calculated from the two integrals:

$$\Phi_1 = -\epsilon_{ff}\sigma^6 N_A\int_{(\sigma/2)-z}^{\sigma}\int_{\sqrt{\sigma^2-y^2}}^{\infty}\rho(y)\frac{2\pi r}{(y^2+r^2)^3}dr dy$$

$$\Phi_2 = -\epsilon_{ff}\sigma^6 N_A\int_{\sigma}^{\infty}\int_{0}^{\infty}\frac{\rho(y)2\pi r}{(y^2+r^2)^3}dr dy$$

$$\Phi = \Phi_1 + \Phi_2.$$

With the local density approximation: $\rho(y) \approx \rho(z)$

$$\Phi = -1/2\,\epsilon_{ff}\sigma^3 N_A\pi\rho(z)\left(\frac{z}{\sigma} + \frac{5}{6}\right).$$

Since a is proportional to Φ, for $0.5\sigma \le z \le 1.5\sigma$, we find

$$\frac{a(z)}{a_{\text{bulk}}} = \frac{\Phi(z)}{\Phi_{\text{bulk}}(\rho(z))} = \left(\frac{5}{16} + \frac{6}{16}\frac{z}{\sigma}\right).$$

For $1.5\sigma \le z < \infty$, the integration is performed in three parts:

$$\Phi_1 = -\epsilon_{ff}\sigma^6 N_A\int_{(\sigma/2)-z}^{-\sigma}\int_{0}^{\infty}\frac{\rho(y)2\pi r}{(y^2+r^2)^3}dr dy$$

$$\Phi_2 = -\epsilon_{ff}\sigma^6 N_A\int_{-\sigma}^{\sigma}\int_{\sqrt{\sigma^2-y^2}}^{\infty}\frac{\rho(y)2\pi r}{(y^2+r^2)^3}dr dy$$

$$\Phi_3 = -\epsilon_{ff}\sigma^6 N_A\int_{\sigma}^{\infty}\int_{0}^{\infty}\frac{\rho(y)2\pi r}{(y^2+r^2)^3}dr dy.$$

With the local density approximation $\rho(y) \approx \rho(z)$ these can be integrated to give

$$\Phi = -\epsilon_{ff}\sigma^3 N_A\pi\rho(z)\left(\frac{4}{3} - \frac{1}{6\left(\frac{z}{\sigma} - \frac{1}{2}\right)^3}\right)$$

$$\frac{a}{a_{\text{bulk}}} = \frac{\Phi}{\Phi_{\text{bulk}}} = \left(1 - \frac{1}{8\left(\frac{z}{\sigma} - \frac{1}{2}\right)^3}\right)$$

and

$$a_{\text{bulk}} = \frac{27}{64}\frac{R^2T_c^2}{P_c} \rightarrow \frac{T_c}{T_{c_{\text{bulk}}}} = \frac{1}{2}.$$

Note that at $z = \sigma/2$, $a = a_{\text{bulk}}/2$, and at $z = \infty$, $a = a_{\text{bulk}}$. Note also that a and its derivative with respect to z are continuous functions at $z = 1.5\sigma$.

Manuscript received Aug. 5, 1993, and revision received May 31, 1994.